Volume 18, Number 1, 2025. pp. 49-59

Jordan Journal of Physics

ARTICLE

Soliton Type Solutions for Electromagnetic Wiggler Free Electron Laser

Mustafa Abu Safa

Department of Applied Physics, Palestine Polytechnic University, Hebron, P. O. Box198, Palestine.

Doi: **https://doi.org/10.47011/18.1.6**

Received on: 11/08/2023; Accepted on: 20/11/2023

Abstract: The nonlinear electromagnetic wave propagation in a system consisting of a relativistic cold-electron beam propagating through an electromagnetic wiggler is solved. A set of coupled nonlinear ordinary differential equations is derived by coordinate transformation to the wiggler coordinates. Soliton-type solutions in the form of coupled electromagnetic and plasma waves are presented numerically, which may represent possible nonlinear saturated states of the electromagnetic wiggler free-electron laser instability. It is shown that the soliton solutions become an eigenvalue problem in the wiggler frequency $\widehat{w}_w$, given a fixed set of parameters $\widehat{w}_c, \gamma_0, \beta, and\ \widehat{\omega}_p$.

Keywords: Solitons, Wiggler, Free Electron Laser, FEL, Undulators.

Introduction

A significant source of mathematical inspiration has been and remains the study of the dynamical behavior of physical systems. In the 20th century, a thorough investigation into many non-linear systems and their commonalities began [1]. Two opposites on the dynamics spectrum have drawn a lot of attention: chaos and solitons. Due to the extremely rich behavior that partial and ordinary differential equations can display, as shown by chaos theory, some deterministic systems can become exponentially unpredictable over time. The soliton hypothesis [2], on the other hand, offers a number of significant instances of non-linear systems behaving in a stable, quasi-linear manner. J. Scott Russell, riding a horse, chased a one-foot-high, thirty-foot-long wave produced by a stopping canal boat traveling at eight to nine miles per hour for nearly two miles in its original form. This was the first experimental demonstration of stable "solitary waves"—the precursors of the term "soliton"—in 1834. In 1895, the KdV problem was solved using this single wave solution [3]. Since then, numerous more nonlinear partial differential equations (PDEs) have featured stable solitary wave solutions prominently, and the techniques for producing soliton solutions have led to numerous profound concepts in both mathematics and science [2, 4].

The free-electron laser, often known as a FEL [5], is a type of laser that, while using some quite different operating principles to create the beam, exhibits many of the same optical characteristics as conventional lasers, including the ability to emit coherent electromagnetic radiation beams with high strength. The lasing medium in free electron lasers is a relativistic electron beam that is free to flow through a wiggler, or transverse periodic magnetic field. The free-electron laser has the broadest frequency range and is the most widely tunable of all laser types. Numerous investigations, including both practical and theoretical ones, have been conducted in recent years on free-electron lasers (FEL) [6]. Various successful findings have been obtained through

Corresponding Author: Mustafa Abu Safa **Email**: mustafa@ppu.edu

experimental and theoretical work at labs and research facilities all around the world [7]. FEL is notable for its unique characteristics, which include its high frequency, high power, and wide bandwidth. Different medical, industrial, and military applications find these properties appealing [8]. A magnetic device called an "undulator" or "wiggler" is typically utilized for passing an electron down, forcing it to follow a periodic oscillatory path in space. This produces the FEL radiation. There are several possible configurations for the wiggler field's precise shape, and both helically and linearly polarized wiggler fields have been used to build FELs [9].

This paper solves the nonlinear electromagnetic wave propagation in a system with a relativistic cold-electron beam moving through an electromagnetic field. A system of coupled nonlinear ODEs has been generated by transforming the coordinates to wiggler coordinates. Numerical solutions of the soliton type, which may reflect potential nonlinear saturated states of the free-electron-laser instability, are shown as coupled electromagnetic and plasma waves.

2. The Electromagnetic Wiggler Field

We start with a relativistic cold fluid to describe the nonlinear evolution of the free electron laser instability [10], [11]. This applies to a relativistic cold electron beam of uniform density propagating in the z-direction through an electromagnetic wiggler field. The electromagnetic wiggler is given by [12], [13]:

$$\vec{E}_w(z,t) = \tilde{E}_w\left[-\hat{e}_x \sin(k_w z + w_w t) + \hat{e}_y \cos(k_w z + w_w t)\right] \tag{1}$$

$$\vec{B}_w(z,t) = -\tilde{B}_w\left[\hat{e}_x \cos(k_w z + w_w t) + \hat{e}_y \sin(k_w z + w_w t)\right], \tag{2}$$

where $\tilde{B}_w = constant, \tilde{E}_w = \frac{w_w \tilde{B}_w}{k_w c}$, and $\lambda_w = \frac{2\pi}{k_w}$ is the wave length, which are derived from the following vector potential:

$$\vec{A}_w(z,t) = A_w\left[\hat{e}_x \cos(k_w z + w_w t) + \hat{e}_y \sin(k_w z + w_w t)\right] \tag{3}$$

where $A_w = \frac{\tilde{B}_w}{k_w}$.

The beam density is assumed to be sufficiently small so that the equilibrium space-charge effects are negligible, and the equilibrium self-magnetic field (B_s) is neglected. Therefore;

$\vec{E}^0(\vec{r}) = \vec{E}_w(z,t)$, $\vec{B}^0(\vec{r}) = \vec{B}_w(z,t)$, and $\vec{A}^0(\vec{r}) = \vec{A}_w(z,t)$.

We consider perturbations in which the spatial variations are one-dimensional in nature with $\frac{\partial}{\partial_x} = \frac{\partial}{\partial_y} = 0$, and $\frac{\partial}{\partial_z}$ is generally nonzero. The perturbed potentials and fields are:

$$\phi(z,t) = \delta\phi(z,t) \tag{4}$$

$$\delta\vec{A}(z,t) = \delta A_x(z,t)\,\hat{e}_x + \delta A_y(z,t)\,\hat{e}_y \tag{5}$$

$$\delta\vec{E}(z,t) = -\frac{1}{c}\frac{\partial}{\partial_z}\delta\phi(z,t)\,\hat{e}_z - \frac{1}{c}\frac{\partial}{\partial_t}\delta A_x(z,t)\,\hat{e}_x - \frac{1}{c}\frac{\partial}{\partial_t}\delta A_y(z,t)\,\hat{e}_y \tag{6}$$

$$\delta\vec{B}(z,t) = -\frac{\partial}{\partial_z}\delta A_y(z,t)\,\hat{e}_x + \frac{\partial}{\partial_z}\delta A_x(z,t)\,\hat{e}_y \tag{7}$$

Thus, the fields become:

$$\vec{E}(\vec{r},t) = \vec{E}^0(z,t) + \delta\vec{E}(z,t) \tag{8}$$

$$\vec{B}(\vec{r},t) = \vec{B}^0(z,t) + \delta\vec{B}(z,t) \tag{9}$$

The vector potential is:

$$\vec{A}(z,t) = \vec{A}^0(z,t) + \delta\vec{A}(z,t) \tag{10}$$

The relativistic momentum and the velocity are related by:

$\vec{p}(\vec{r},t) = \gamma m\vec{v}$, where $\gamma = (1 + \frac{p^2}{m^2c^2})^{1/2}$ is the relativistic factor and $\vec{v}(\vec{r},t)$ is the flow velocity.

The continuity equation is given by:

$\frac{\partial n}{\partial t} + \frac{\partial(nv_z)}{\partial z} = 0$,

where $n(z,t)$ is the number density.

The equation of motion for a fluid element is:

$$\frac{d\vec{P}}{dt} = -e\left[\vec{E} + \frac{1}{c}\vec{v}\times\vec{B}\right], \tag{11}$$

where the convective derivative is: $\frac{d}{dt} = \frac{\partial}{\partial t} + v_z\frac{\partial}{\partial z}$.

$$\vec{E} = -\frac{\partial}{\partial z}\delta\phi(z,t)\,\hat{e}_z - \frac{1}{c}\frac{\partial}{\partial t}\vec{A} \tag{12}$$

Substituting into Eq. (11) gives:

$$\frac{d\vec{P}_\perp}{dt} = -e\left[-\frac{1}{c}\frac{\partial}{\partial t}\vec{A}_\perp + \frac{1}{c}\{\vec{v}\times(\nabla\times\vec{A})\}_\perp\right] \tag{13}$$

$$\{\vec{v}\times(\nabla\times\vec{A})\}_\perp = -v_z\frac{\partial}{\partial z}\vec{A}_\perp \tag{14}$$

$$\frac{d\vec{P}_\perp}{dt} = \frac{e}{c}\left[\frac{\partial}{\partial t}\vec{A}_\perp + v_z\frac{\partial}{\partial z}\vec{A}_\perp\right] = \frac{e}{c}\frac{d\vec{A}}{dt} \tag{15}$$

Or, $\frac{d}{dt}\left[\vec{P}_\perp - \frac{e}{c}\vec{A}\right] = 0$ (16)

Now, integrating yields:

$$\int \frac{d}{dt}\left[\vec{P}_\perp - \frac{e}{c}\vec{A}\right] = constant \tag{17}$$

Assuming the constant to be zero, we conclude:

$$\left[\vec{P}_\perp - \frac{e}{c}\vec{A}\right] = 0 \Rightarrow \vec{P}_\perp = \frac{e}{c}\vec{A} \tag{18}$$

The wave equation for $\vec{A}$ (choosing Coulomb's gauge) is written as:

$$\nabla^2\vec{A} - \frac{1}{c^2}\frac{\partial^2}{\partial t^2}\vec{A} = -\frac{4\pi}{c}\vec{J}_\perp \tag{19}$$

$$\vec{J}_\perp = -ne\,\vec{v}_\perp = \frac{-ne\,\vec{P}_\perp}{m\gamma} = \frac{-ne^2\vec{A}}{m\gamma c} \tag{20}$$

$$\left[\frac{\partial^2}{\partial z^2} - \frac{1}{c^2}\frac{\partial^2}{\partial t^2}\right]\delta\vec{A} = \frac{4\pi e^2}{mc^2}\left[\frac{n}{\gamma}\vec{A} - \frac{n_0}{\gamma_0}\vec{A}^0\right] = \frac{\omega_{p0}^2}{c^2}\left[\frac{n}{n_0}\frac{\vec{A}}{\gamma} - \frac{\vec{A}^0}{\gamma_0}\right] \tag{21}$$

Back to the equation of motion with its z-component:

$$\frac{\partial p_z}{\partial t} + v_z\frac{\partial p_z}{\partial z} = -e\left[E_z + \frac{1}{c}(\vec{v}\times\vec{B})_z\right] \tag{22}$$

while the $E_z = -\frac{\partial}{\partial z}\phi(z,t)$ and

$$\left(\vec{v}\times\vec{B}\right)_z = \left(v_xB_y - v_yB_x\right) = v_x\frac{\partial}{\partial z}A_x - v_y\frac{\partial}{\partial z}A_y$$

$$= \frac{c}{e}v_x\frac{\partial}{\partial z}p_x + \frac{c}{e}v_y\frac{\partial}{\partial z}p_y \tag{23}$$

Then,

$$\frac{\partial p_z}{\partial t} = e\frac{\partial}{\partial z}\phi - \left[\frac{p_x}{m\gamma}\frac{\partial}{\partial z}p_x + \frac{p_y}{m\gamma}\frac{\partial}{\partial z}p_y + \frac{p_z}{m\gamma}\frac{\partial}{\partial z}p_z\right] = e\frac{\partial}{\partial z}\phi - mc^2\frac{\partial}{\partial z}\gamma \tag{24}$$

Differentiation with respect to t:

$$\frac{\partial^2 p_z}{\partial t^2} = e\frac{\partial^2}{\partial t\partial z}\phi - mc^2\frac{\partial^2}{\partial t\partial z}\gamma \tag{25}$$

Now, using the axial components of Maxwell's equations:

$$\nabla\times\delta\vec{B} = \frac{4\pi}{c}\delta\vec{J} + \frac{1}{c}\frac{\partial}{\partial t}\delta\vec{E} \tag{26}$$

But, $(\nabla\times\delta\vec{B})_z = \left(\partial_x\delta B_y - \partial_y\delta B_x\right) = 0 - 0 = 0.$

Then, $\frac{\partial}{\partial t}\delta E_z = -4\pi(J_z - J_{0z}) = 4\pi e(nv_z - n_0v_{0z}).$

$$\frac{\partial}{\partial t}\left(-\frac{\partial}{\partial z}\delta\phi\right) = -\frac{\partial}{\partial t}\left(\frac{\partial}{\partial z}\phi\right) = -\left(\frac{\partial^2}{\partial t\partial z}\phi\right) = 4\pi e(nv_z - n_0v_{0z}) \tag{27}$$

Using $\vec{p} = \gamma m\vec{v}$ and substituting into Eq. (27), we get:

$$e\frac{\partial^2}{\partial t\partial z}\phi = -\frac{4\pi e^2 n_0}{m}\left[\frac{n}{n_0}\frac{p_z}{\gamma} - \frac{p_{0z}}{\gamma_0}\right] \tag{28}$$

Substituting into Eq. (25) gives:

$$\frac{\partial^2 p_z}{\partial t^2} = -mc^2\frac{\partial^2\gamma}{\partial t\partial z} - \omega_{p0}^2\left[\frac{n}{n_0}\frac{p_z}{\gamma} - \frac{p_{0z}}{\gamma_0}\right] \tag{29}$$

3. Transforming to the Wiggler Coordinates Frame

$$\hat{e}_1 = \hat{e}_x\cos(k_wz + w_wt) + \hat{e}_y\sin(k_wz + w_wt),$$

$$\hat{e}_2 = -\hat{e}_x\sin(k_wz + w_wt) + \hat{e}_y\cos(k_wz + w_wt),\ \hat{e}_3 = \hat{e}_z$$

Equation (3) becomes:

$$A_x = A_1\cos(k_wz + w_wt) - A_2\sin(k_wz + w_wt) \tag{30}$$

$$A_y = A_1\sin(k_wz + w_wt) + A_2\cos(k_wz + w_wt) \tag{31}$$

$$A_z = A_3 \tag{32}$$

Substituting into the wave equation, we get:

$$\left[\frac{\partial^2}{\partial z^2} - \left(k_w^2 - \frac{w_w^2}{c^2}\right) - \frac{1}{c^2}\frac{\partial^2}{\partial t^2}\right]\delta A_1 - 2\left[k_w\frac{\partial}{\partial z} - \frac{w_w}{c}\frac{1}{c}\frac{\partial}{\partial t}\right]\delta A_2 = \frac{\omega_{p0}^2}{c^2}\left[\frac{n}{n_0}\frac{A_1}{\gamma} - \frac{A_1^0}{\gamma_0}\right] \tag{33}$$

$$\left[\frac{\partial^2}{\partial z^2} - \left(k_w^2 - \frac{w_w^2}{c^2}\right) - \frac{1}{c^2}\frac{\partial^2}{\partial t^2}\right]\delta A_2 + 2\left[k_w\frac{\partial}{\partial z} - \frac{w_w}{c}\frac{1}{c}\frac{\partial}{\partial t}\right]\delta A_1 = \frac{\omega_{p0}^2}{c^2}\left[\frac{n}{n_0}\frac{A_2}{\gamma}\right] \tag{34}$$

Making the traveling wave ansatz, where all the dynamical quantities depend on z and t by the combination $\xi = z - ut$, *so* $\frac{\partial}{\partial z} = \frac{d}{d\xi}$, *and* $\frac{\partial}{\partial t} = -u\frac{d}{d\xi}$.

Substituting into the wave equation, we obtain the following form in the wave frame:

$$\frac{\partial}{\partial t}n + \frac{\partial}{\partial z}(nv_z) = 0$$

$$-u\frac{dn}{d\xi} + n\frac{dv_z}{d\xi} + v_z\frac{dn}{d\xi} = 0$$

$$(v_z - u)\frac{dn}{d\xi} = -n\frac{dv_z}{d\xi}$$

$$-\frac{dn}{n} = \frac{dv_z}{(v_z - u)} \tag{35}$$

Integrating:

$$\ln\left(\frac{n}{n_0}\right) = -\ln\left(\frac{v_z-u}{v_{0z}-u}\right) \tag{36}$$

Normalizing as follows: $\beta \equiv \frac{u}{c}$, $\beta_b \equiv \frac{v_0}{c}$, $\varrho_3 \equiv \frac{p_z}{mc}$:

$$\frac{n}{n_0} = \frac{v_{0z}/c-u/c}{v_z/c-u/c} = \gamma\left(\frac{\beta_b-\beta}{\gamma\left(\frac{mv_z}{mc}\right)-\gamma\beta}\right) \tag{37}$$

$$\frac{n}{n_0} = \gamma\left(\frac{\beta-\beta_b}{\gamma\beta-\varrho_3}\right) \tag{38}$$

Equation (33) can be reduced to the following form:

$$u^2\ \frac{d^2p_z}{d\xi^2} = mc^2u\frac{d^2\gamma}{d\xi^2} \quad -\omega_{p0}^2\left[\frac{n}{n_0}\frac{p_z}{\gamma}-\frac{p_{0z}}{\gamma_0}\right] \tag{39}$$

$$\beta\ \frac{d^2(\beta\,\varrho_3-\gamma)}{d\eta^2}+\widehat{\omega}_p^2\left[\frac{n}{n_0}\frac{\varrho_3}{\gamma}-\frac{\varrho_{03}}{\gamma_0}\right]=0 \tag{40}$$

where $\xi = \eta/k_w, p_z = \varrho_3 mc, \omega_{p0}^2 = \widehat{\omega}_p\ ck_w$.

And in terms of ϱ_1, ϱ_2 and $Z = (\beta\,\varrho_3 - \gamma)$:

$$(\gamma\beta - \varrho_3) = \sqrt{(\beta^2-1)(1+\varrho_1{}^2+\varrho_2{}^2)+Z^2} \tag{41}$$

We can rewrite Eq. (38) as follows:

$$\frac{n}{n_0\gamma} = \frac{|\beta-\beta_b|}{\sqrt{(\beta^2-1)(1+\varrho_1{}^2+\varrho_2{}^2)+Z^2}} \tag{42}$$

Or, $$\frac{n\,\varrho_3}{n_0\gamma} = \left(\frac{\beta-\beta_b}{\beta^2-1}\right)+\frac{n}{n_0\gamma}\left(\frac{\beta Z}{\beta^2-1}\right) \tag{43}$$

Hence,

$$\frac{n\,\varrho_3}{n_0\gamma} = \left(\frac{\beta-\beta_b}{\beta^2-1}\right)+\left(\frac{\beta|\beta-\beta_b|\,Z}{(\beta^2-1)\sqrt{(\beta^2-1)(1+\varrho_1{}^2+\varrho_2{}^2)+Z^2}}\right) \tag{44}$$

Substitution into Eq. (40) gives:

$$\beta\ \frac{d^2Z}{d\eta^2}+\widehat{\omega}_p^2\left[\left(\frac{\beta-\beta_b}{\beta^2-1}\right)+\left(\frac{\beta|\beta-\beta_b|\,Z}{(\beta^2-1)\sqrt{(\beta^2-1)(1+\varrho_1{}^2+\varrho_2{}^2)+Z^2}}\right)-\frac{\varrho_{03}}{\gamma_0}\right]=0$$

Finally, the differential equation of Z is:

$$Z''+\frac{\widehat{\omega}_p^2\gamma_0|\beta-\beta_b|\,Z}{(\beta^2-1)\sqrt{(\beta^2-1)(1+\varrho_1{}^2+\varrho_2{}^2)+Z^2}}+\frac{\widehat{\omega}_p^2\gamma_0(1-\beta_b\beta)}{(\beta^2-1)}=0 \tag{45}$$

where the over prime denotes $\frac{d}{d\eta}$.

Again, using the combination of the variables z and t by $\xi = z-ut$, where u = constant is the signal speed, $\frac{\partial}{\partial z}=\frac{d}{d\xi}$, and $\frac{\partial}{\partial t}=-u\frac{d}{d\xi}$. Substituting into and simplifying Eq. (33), we get:

$$\frac{d^2\delta A_1}{d\xi^2}-\frac{u^2}{c^2}\frac{d^2\delta A_1}{d\xi^2}\quad-\left(k_w^2-\frac{w_w^2}{c^2}\right)\delta A_1-2\left(k_w\frac{d\,\delta A_2}{d\,\xi}+\frac{w_w}{c}\frac{u}{c}\frac{d\,\delta A_2}{d\,\xi}\right)=\frac{\omega_{p0}^2}{c^2}\left[\frac{n}{n_0}\frac{A_1}{\gamma}-\frac{A_1^0}{\gamma_0}\right] \tag{46}$$

Using $\xi=\frac{\eta}{k_w}, \delta A_1=\frac{mc^2}{e}\delta\,\varrho_1$, $\delta A_2=\frac{mc^2}{e}\delta\,\varrho_2$, $\widehat{\omega}_{p0}^2=\widehat{\omega}_p^2\gamma_0, \widehat{w}_w=\frac{w_w}{c\,k_w}$ and in terms of ϱ_1, ϱ_2 and $Z=(\beta\,\varrho_3-\gamma)$, Eq. (46) can be reduced to the following form:

$$(1-\beta^2)\delta\varrho_1''-(1-\widehat{w}_w^2)\delta\,\varrho_1-2(1+\beta\,\widehat{w}_w)\delta\varrho_2'=\widehat{\omega}_p^2\gamma_0\left[\frac{n}{n_0}\frac{\varrho_1}{\gamma}-\frac{\varrho_{01}}{\gamma_0}\right] \tag{47}$$

We can reduce the above equation using: $\delta\varrho_1=\varrho_1-\varrho_{01}$, $\delta\varrho_1'=\varrho_1'-\varrho_{01}'$, $\delta\varrho_1''=\varrho_1''-\varrho_{01}''$, and $\delta\varrho_2=\varrho_2$, $\delta\varrho_2'=\varrho_2'$, $\delta\varrho_2''=\varrho_2''$, since $\varrho_{01}=\frac{P_1}{mc}=\frac{e\hat{B}}{mc^2k_w}$ then, $\varrho_{01}'=\varrho_{01}''=0$,

$$(1-\beta^2)\varrho_1''-\left[(1-\widehat{w}_w^2)+\widehat{\omega}_p^2\gamma_0\frac{n}{n_0\gamma}\right]\varrho_1-2(1+\beta\,\widehat{w}_w)\varrho_2'=-\widehat{\omega}_p^2\gamma_0\frac{\varrho_{01}}{\gamma_0}.$$

Now substituting $\frac{\varrho_{01}}{\gamma_0}=\frac{P_1}{mc\gamma_0}=\frac{e\hat{B}}{mc^2k_w\gamma_0}=\widehat{w}_c$, and $\frac{n}{n_0\gamma}=\frac{|\beta-\beta_b|}{\sqrt{(\beta^2-1)(1+\varrho_1{}^2+\varrho_2{}^2)+Z^2}}$ yields:

$$(1-\beta^2)\varrho_1''-\left[(1-\widehat{w}_w^2)+\widehat{\omega}_p^2\gamma_0\frac{|\beta-\beta_b|}{\sqrt{(\beta^2-1)(1+\varrho_1{}^2+\varrho_2{}^2)+Z^2}}\right]\varrho_1-2(1+\beta\,\widehat{w}_w)\varrho_2'=-\widehat{\omega}_p^2\gamma_0\widehat{w}_c \tag{48}$$

Similarly, Eq. (41) becomes:

$$(1-\beta^2)\varrho_2''-\left[(1-\widehat{w}_w^2)+\widehat{\omega}_p^2\gamma_0\frac{|\beta-\beta_b|}{\sqrt{(\beta^2-1)(1+\varrho_1{}^2+\varrho_2{}^2)+Z^2}}\right]\varrho_2+2(1+\beta\,\widehat{w}_w)\varrho_1'=0 \tag{49}$$

4. Results and Discussion

Equations (45), (47), and (48) are the final set of nonlinear coupled equations that we will solve to study the nonlinear evolution of the electromagnetic wiggler FEL.

The equilibrium solutions ($\frac{d}{d\,\eta} = 0$) are given for Eqs. (45), (47), and (48) as:

$\varrho_{01} = \frac{\gamma_0 \widehat{w}_c(1+\widehat{\omega}_p^2)}{(1+\widehat{\omega}_p^2)-\widehat{w}_w^2}$, $\quad \varrho_{02} = 0$, $\quad$ and $\quad Z_0 = \gamma_0(\,\beta_b\beta - 1)$.

The small-signal analysis around the equilibrium [10] yields a traveling wave dispersion relation, which can be related formally to the familiar cold fluid mode dispersion relation for an electromagnetic wiggler free electron laser. It was shown by Davidson, Johnston, and Sen [10] that the free electron laser instability corresponds to the condition $\beta < \beta_b < 1$.

The solutions can be infinite wave trains, solitons, or periodic chaotic. In our case, we are addressing the soliton solutions for which we solved Eqs. (45), (47), and (48) numerically. Such solutions for the electromagnetic wiggler FEL are evident in the profiles of $\delta\,\varrho_1\,, \delta\,\varrho_2, \delta Z, and\ \frac{n}{n_0\gamma}$.

Figure 1(a) shows a soliton-type solution for $\widehat{w}_c = 0.50, \gamma_0 = 10.0, \beta = 0.50, \widehat{\omega}_p = 0.501935$, and $\widehat{w}_w = 0.00$, representing the case without an electromagnetic wiggler. The $\delta Z = Z - Z_0$ profile is bell-shaped, while the other profiles ($\delta\,\varrho_1\,, \delta\,\varrho_2, and\ \frac{n}{n_0\gamma}$) have a number of nodes, as seen in Figs. 1(b), 1(c), and 1(d). The δZ profile has a maximum amplitude of about -6.0, whereas the $\frac{n}{n_0\gamma}$ profile remains positive, as expected, with density reduced across most of the region but sharply increasing at the edges.

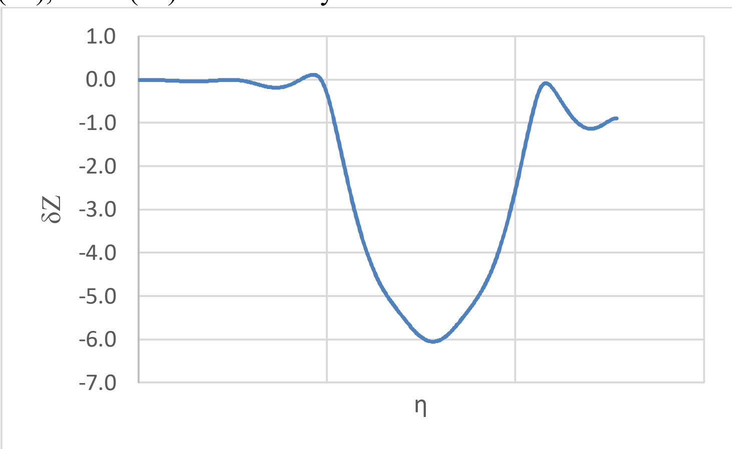

FIG. 1(a). Profile of δZ for a soliton pulse with $\widehat{w}_w = 0.00$, $\widehat{w}_c = 0.50$, $\gamma_0 = 10.0, \beta = 0.50, and\ \widehat{\omega}_p = 0.501935$.

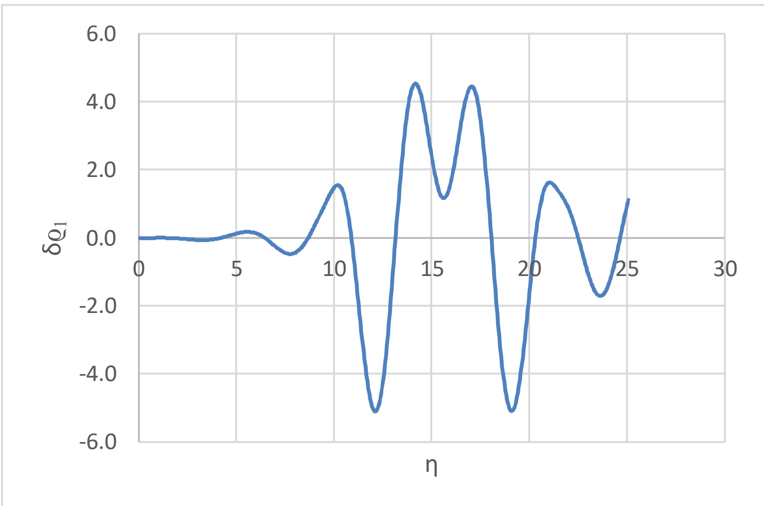

FIG. 1(b). Profile of $\delta\,\varrho_1$ for a soliton pulse with $\widehat{w}_w = 0.00$, $\widehat{w}_c = 0.50, \gamma_0 = 10.0, \beta = 0.50, and\ \widehat{\omega}_p = 0.501935$.

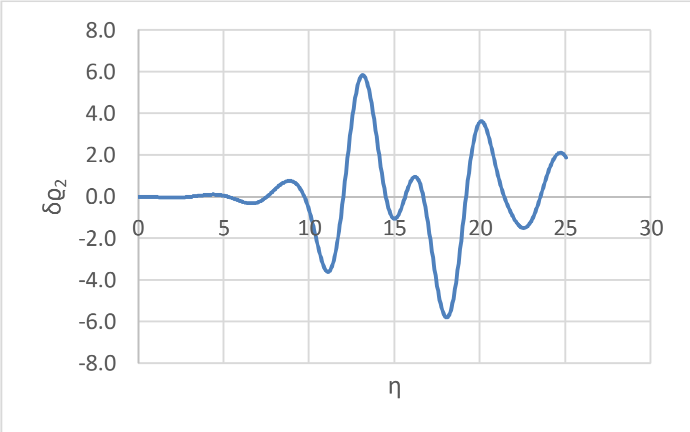

FIG. 1(c). Profile of $\delta\,\varrho_2$ for a soliton pulse with $\widehat{w}_w = 0.00, \widehat{w}_c = 0.50, \gamma_0 = 10.0, \beta = 0.50, and\ \widehat{\omega}_p = 0.501935.$

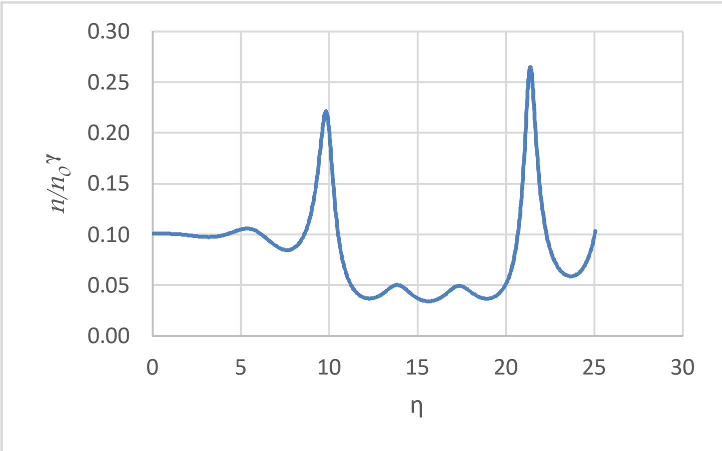

FIG. 1(d). Profile of $\frac{n}{n_0\gamma}$ for a soliton pulse with $\widehat{w}_w = 0.00, \widehat{w}_c = 0.50, \gamma_0 = 10.0, \beta = 0.50, and\ \widehat{\omega}_p = 0.501935.$

Figures 2(a), 2(b), 2(c), and 2(d) show a soliton-type solution for $\widehat{w}_c = 0.50, \gamma_0 = 10.0,$ $\beta = 0.50,$ $\widehat{\omega}_p = 0.501935,$ $and\ \widehat{w}_w = 0.50$ (in the presence of the electromagnetic wiggler). The $\delta Z = Z - Z_0$ profile retains its bell shape, while the other profiles $(\delta\,\varrho_1, \delta\,\varrho_2, and\ \frac{n}{n_0\gamma})$ exhibit multiple nodes. The δZ profile has a maximum amplitude of about -5.0 but is shifted to the left, as seen in the figure (appears earlier). Meanwhile, the $\frac{n}{n_0\gamma}$ profile remains positive, showing a reduction in density over most of the region, though the depleted region is wider in this case.

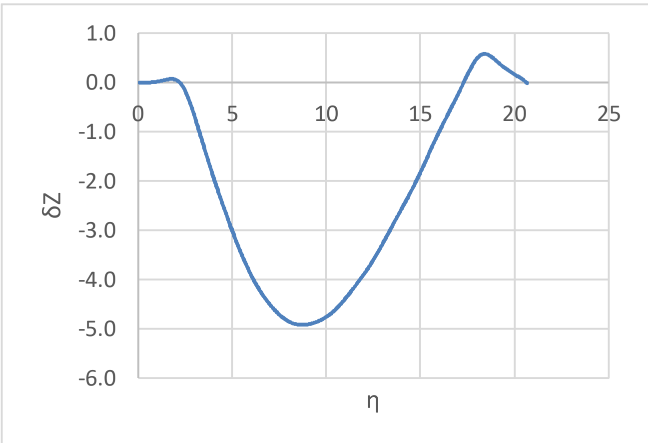

FIG. 2(a). Profile of δZ for a soliton pulse with $\widehat{w}_w = 0.50, \widehat{w}_c = 0.50, \gamma_0 = 10.0, \beta = 0.50, and\ \widehat{\omega}_p = 0.501935.$

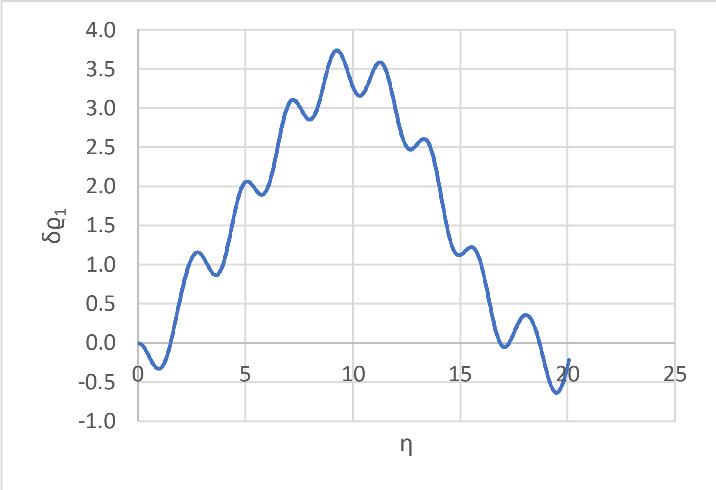

FIG. 2(b). Profile of $\delta\, \varrho_1$ for a soliton pulse with $\widehat{w}_w = 0.50$, $\widehat{w}_c = 0.50$, $\gamma_0 = 10.0, \beta = 0.50, and\ \widehat{\omega}_p = 0.501935$.

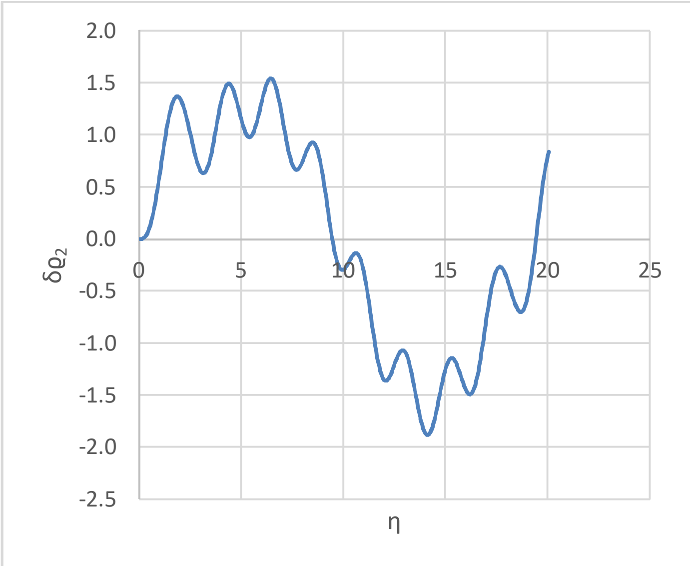

FIG. 2(c). Profile of $\delta\, \varrho_2$ for a soliton pulse with $\widehat{w}_w = 0.50$, $\widehat{w}_c = 0.50$, $\gamma_0 = 10.0, \beta = 0.50, and\ \widehat{\omega}_p = 0.501935$.

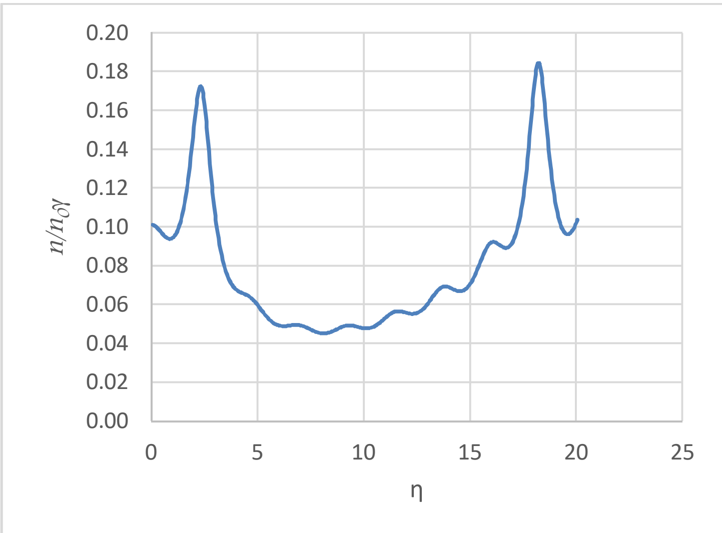

FIG. 2(d). Profile of $\frac{n}{n_0\gamma}$ for a soliton pulse with $\widehat{w}_w = 0.50$, $\widehat{w}_c = 0.50$, $\gamma_0 = 10.0, \beta = 0.50, and\ \widehat{\omega}_p = 0.501935$.

Figures 3(a), 3(b), 3(c), and 3(d) show the soliton solution for $\widehat{w}_c = 0.60$, $\gamma_0 = 10.0$, $\beta = 0.50$, $\widehat{\omega}_p = 0.501935, and\ \widehat{w}_w = 0.60$ (in the presence of the electromagnetic wiggler). The $\delta Z = Z - Z_0$ is still bell-shaped, while the other profiles ($\delta\,\varrho_1, \delta\,\varrho_2, and\ \frac{n}{n_0\gamma}$) have a number of nodes. The δZ profile has a maximum amplitude of about -7.0, which is greater than that observed for $\widehat{w}_w = 0.50$, while the $\frac{n}{n_0\gamma}$ profile behaves almost identically.

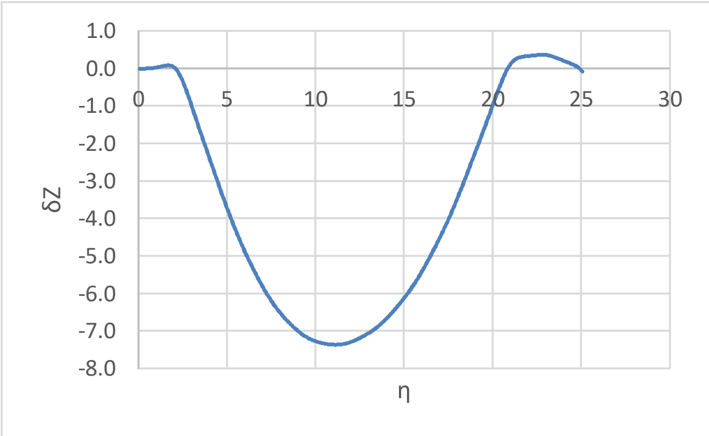

FIG. 3(a). Profile of δZ for a soliton pulse with $\widehat{w}_w = 0.60, \widehat{w}_c = 0.50, \gamma_0 = 10.0, \beta = 0.50, and\ \widehat{\omega}_p = 0.501935$.

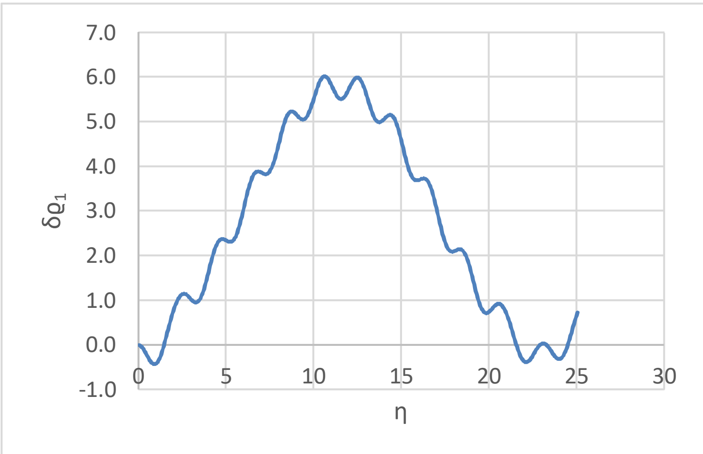

FIG. 3(b). Profile of $\delta\,\varrho_1$ for a soliton pulse with $\widehat{w}_w = 0.60,\ \widehat{w}_c = 0.50, \gamma_0 = 10.0, \beta = 0.50, and\ \widehat{\omega}_p = 0.501935$.

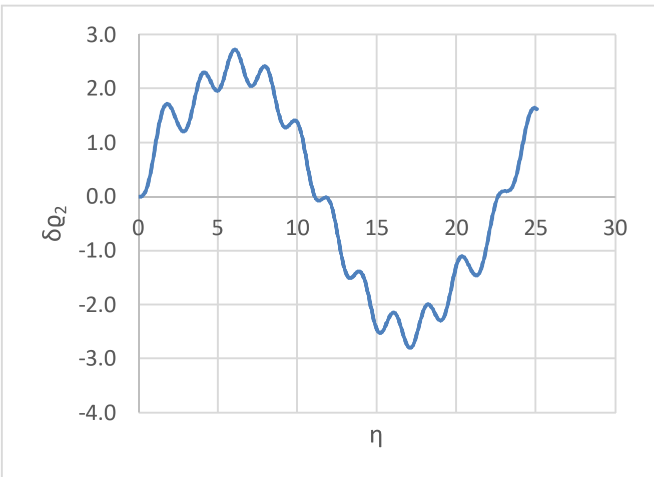

FIG. 3(c). Profile of $\delta\,\varrho_2$ for a soliton pulse with $\widehat{w}_w = 0.60, \widehat{w}_c = 0.50, \gamma_0 = 10.0, \beta = 0.50, and\ \widehat{\omega}_p = 0.501935$.

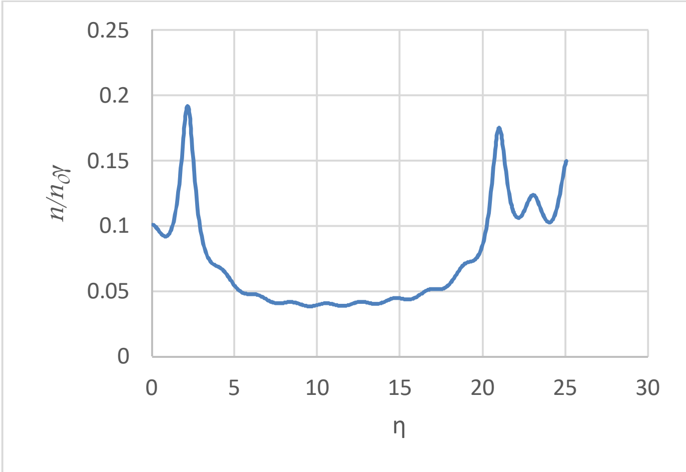

FIG. 3(d). Profile of $\frac{n}{n_0\gamma}$ for a soliton pulse with $\widehat{w}_w = 0.60, \widehat{w}_c = 0.50, \gamma_0 = 10.0, \beta = 0.50, and\ \widehat{\omega}_p = 0.501935$.

Finally, Figs. 4(a), 4(b), 4(c), and 4(d) show the soliton solution for $\widehat{w}_c = 0.60, \gamma_0 = 10.0$, $\beta = 0.50$, $\widehat{\omega}_p = 0.501935, and\ \widehat{w}_w = 0.70$, (in the presence of the electromagnetic wiggler). The $\delta Z = Z - Z_0$ profile remains bell-shaped, while the other profiles ($\delta\,\varrho_1, \delta\,\varrho_2, and\ \frac{n}{n_0\gamma}$) exhibit multiple nodes. The δZ profile has a maximum amplitude of about -12.0, which is greater than that observed for $\widehat{w}_w = 0.60$.

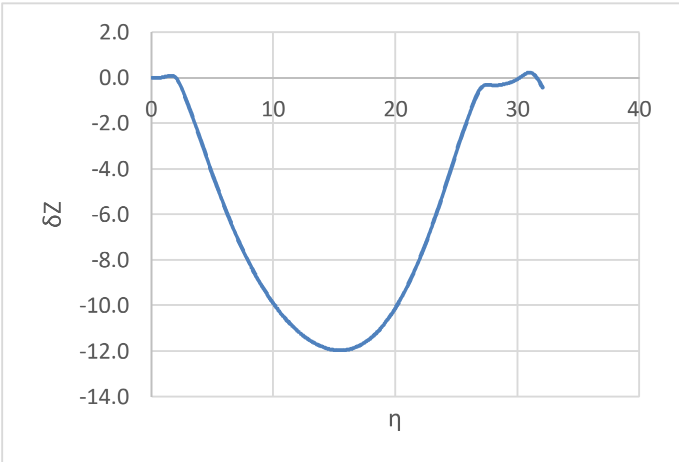

FIG. 4(a). Profile of δZ for a soliton pulse with $\widehat{w}_w = 0.70, \widehat{w}_c = 0.50, \gamma_0 = 10.0, \beta = 0.50, and\ \widehat{\omega}_p = 0.501935$.

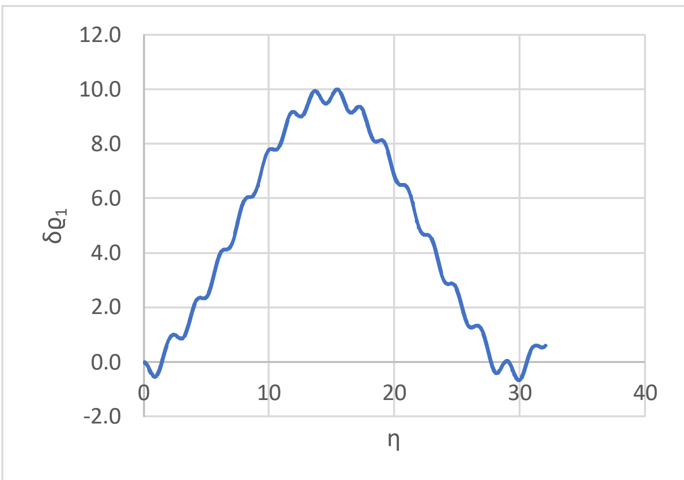

FIG. 4(b). Profile of $\delta\,\varrho_1$ for a soliton pulse with $\widehat{w}_w = 0.70, \widehat{w}_c = 0.50, \gamma_0 = 10.0, \beta = 0.50, and\ \widehat{\omega}_p = 0.501935$.

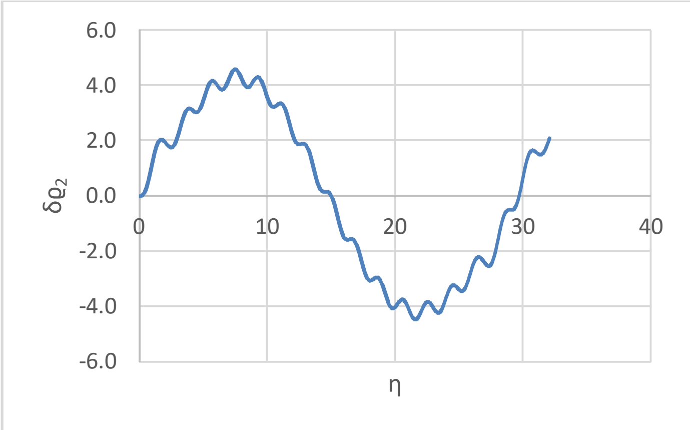

FIG. 4(c). Profile of $\delta\, \varrho_2$ for a soliton pulse with $\widehat{w}_w = 0.70, \widehat{w}_c = 0.50, \gamma_0 = 10.0, \beta = 0.50, and\ \widehat{\omega}_p = 0.501935$.

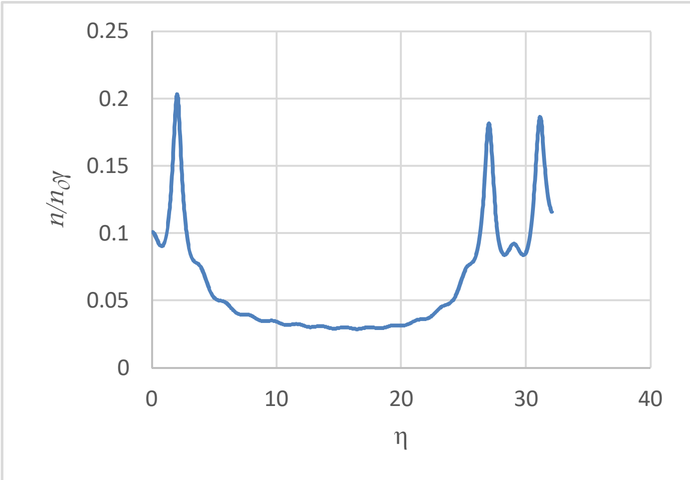

FIG. 4(d). Profile of $\frac{n}{n_0\gamma}$ for a soliton pulse with $\widehat{w}_w = 0.70, \widehat{w}_c = 0.50, \gamma_0 = 10.0, \beta = 0.50, and\ \widehat{\omega}_p = 0.501935$.

5. Conclusion

To conclude, I have obtained a soliton solution for the electromagnetic wiggler free-electron laser. The one-dimensional nonlinear traveling wave solutions were obtained by a numerical solution of the relativistic equations in the form of isolated pulses of coupled electromagnetic and plasma waves. It is shown that the soliton solutions became an eigenvalue problem in the wiggler frequency $\widehat{w}_w$ for a fixed set of parameters $\widehat{w}_c, \gamma_0, \beta, and\ \widehat{\omega}_p$. This new class of solutions has a variety of potential applications and may represent nonlinear saturated states of the electromagnetic wiggler free-electron-laser instability.

References:

[1] Hirota, R., "The Direct Method in Soliton Theory", (Cambridge University Press, 2004).

[2] Manukure, S. and Booker, T., Partial Differ. Equ. Appl. Math., 4 (2021) 100140.

[3] Drazin, P.G. and Johnson, R.S., "Solitons: An Introduction", (Cambridge University Press, 1989).

[4] Al-Ghafri, K.S., Waves Random Complex Media, 28 (2) (2018) 261.

[5] Udholm, P., Willett, J.E., and Bilikmen, S., J. Phys. D, 24 (1991) 1278.

[6] Marshall, T.C., "Free Electron Laser", (New York, Macmillan, 1985).

[7] Bilikmen, S. and Abu Safa, M., Tr. J. Phys., (16) (1992) 537.

[8] Schmitt, W.J. and Elliott, C.J., Phys. Rev. A, 41 (1990) 3853.

[9] Abu Safa, M., Int. J. Phys. Sci., 9 (21) (2014) 459.

[10] Davidson, R.C., Johnston, G.L., and Sen, A., Phys. Rev. A, 34 (1986) 392.

[11] Sen, A. and Johnston, G.L., Phys. Rev. Lett., (70) (1993) 786.

[12] Fruend, H.P., Kehs, R.A., and Granatstein, V.L., Phys. Rev. A, 34 (1986) 2007.

[13] Fruend, H.P. et al., IEEE J. Quantum Electron., QE 21 (7) (1985) 1080.